Infrared transient grating measurements of the dynamics of hydrogen local mode vibrations in amorphous silicon-germanium

K. W. Jobson and J.-P. R. Wells[a)]
Department of Physics and Astronomy, University of Sheffield, Sheffield S3 7RH, United Kingdom

R. E. I. Schropp
Department of Physics and Astronomy, University of Utrecht, P.O. Box 80000, TA 3508 Utrecht, The Netherlands

N. Q. Vinh
FELIX Free Electron Laser Facility, FOM Institute for Plasmaphysics "Rijnhuizen," P.O. Box 1207, 3430 BE, Nieuwegein, The Netherlands

J. I. Dijkhuis
Department of Physics and Astronomy, University of Utrecht, P.O. Box 80000, TA 3508 Utrecht, The Netherlands

(Received 6 June 2007; accepted 22 October 2007; published online 7 January 2008)

We report on picosecond, time-resolved measurements of the vibrational relaxation and decay pathways of the Si–H and Ge–H stretching modes in hydrogenated amorphous silicon-germanium thin films (*a*-SiGe:H). It is demonstrated that the decay of both modes has a nonexponential shape, attributable to the local environment of the Si–H and Ge–H bonds. Temperature dependent measurements of the ensemble averaged population decay time $\langle T_1 \rangle$ are used to demonstrate that the stretch modes relax to Si(Ge)-H bending modes and that the excess energy is dissipated into a combination of bulk vibrations. The influence of the mixed character Si-Ge bulk vibrations upon the relaxation dynamics is discussed. © *2008 American Institute of Physics*. [DOI: 10.1063/1.2822337]

I. INTRODUCTION

Hydrogenated amorphous silicon (*a*-Si:H) is widely regarded as the prototypical amorphous material and as a consequence has been intensely investigated for many years. Thanks to the relative ease with which large area films of *a*-Si:H can be manufactured, it has found many applications in the optoelectronics industry, in particular for solar cell technologies. An important aspect of *a*-Si:H films used in this context is the ability to tune the band gap to longer wavelengths by incorporating germanium into the film during deposition, resulting in the creation of hydrogenated amorphous silicon-germanium (*a*-SiGe:H) films. The desired band gap energy can be readily engineered as it depends linearly upon the molar fraction of germanium deposited into the film.[1] Thus by utilizing multijunction solar cell designs, where the band gap of each individual solar cell is tailored to specific bands of the solar spectrum, the overall spectral response of the device can be improved.

However, there are significant drawbacks to alloying *a*-Si:H films. The optoelectronic properties of *a*-SiGe:H films are generally worse than device quality *a*-Si:H films. The photoconductive response of *a*-SiGe:H films deteriorates with increasing germanium content,[2] deposition of *a*-SiGe:H layers under the same conditions as those used for preparing device-quality *a*-Si:H layers causes increased concentration of midgap defect states[3] (though it must be pointed out that later work has shown that films of *a*-SiGe:H with lower gap- and tail-state concentrations can be fabricated through deposition under low-pressure, high ion flux conditions[4]) and the Staebler–Wronski effect (light-induced degradation of the film's optoelectronic properties) is also observed in *a*-SiGe:H films with higher germanium content.[5]

Time-resolved mid-infrared spectroscopy is emerging as a powerful tool for the study of the dynamics of localized vibrational modes in solids. These experiments provide new and unique ways of gathering information on not only the dynamics of the localized mode, but also the structural properties of the environment in which the vibrational mode resides. The field itself has grown concurrently with the development of midinfrared laser sources: formerly the development of free electron lasers (FELs) and more latterly the growing availability of table-top optical parametric amplifiers. In this work we have taken advantage of the Dutch FEL—FELIX—in order to provide the ~5.00 μm optical wavelength pulses required for these transient grating measurements.

In the present study, samples of *a*-SiGe:H were grown by the plasma enhanced chemical vapor deposition (PECVD) method and transient grating experiments were performed on the Si-H and Ge-H stretching modes of the Si(Ge):H complexes. The results garnered from the present study build on past data gathered from studying the dynamics of Si-H and Ge-H vibrations in their "native" environment [i.e., the Si-H stretching vibration in *a*-Si:H (Refs. 6 and 7) and the Ge-H stretching vibration in *a*-Ge:H (Ref. 8)]. In these systems it was observed that the decay of the transient grating signal

[a)]Author to whom correspondence should be addressed. Present address: Department of Physics and Astronomy, University of Canterbury, PB4800, Christchurch 8020, New Zealand. Electronic mail: jon-paul.wells@canterbury.ac.nz. FAX: +64 (0)3 3642469.

generated from resonantly exciting the Si/Ge-H stretch mode had a nonexponential shape that was demonstrated to stem from the strong coupling of the highly localized Si/Ge-H mode to the surrounding amorphous environment, leading to a distribution of T_1 decay times. Interestingly, this is not the case for either Si-D stretch modes in *a*-Si:D (Ref. 9) or for Si-O-Si asymmetric stretching modes in *a*-Si:$O_{0.1}$.[10] In the case of *a*-SiGe:H, both the Si-H and Ge-H localized modes are coupled to the same phonon bath, but the bath differs from that which is present when the Si(Ge):H complexes are located in the native environment by introducing mixed long-wavelength Si-Ge vibrational states[2] that can be decayed into. These mixed character vibrations are highly prominent in the vibrational density of states of *a*-SiGe:H thin films and can be easily distinguished from states belonging to the Si(Ge) transverse optical (TO) modes due to the large mass difference between the Si and Ge atoms. The effect of these extra states in the phonon bath should manifest themselves in the relaxation dynamics of the localized vibrational modes (LVMs).

II. EXPERIMENTAL DETAILS

The samples consist of thin films of *a*-SiGe:H that were prepared on *c*-Si substrates by PECVD. The films were measured to have a thickness of ~1 μm. The infrared absorption of the films was measured by use of a Fourier-transform infrared spectrometer. The transient grating measurements were performed by using the Dutch free electron laser (FELIX) in Nieuwegein. FELIX provides 6 μs duration macropulses at a 5 Hz repetition rate which are composed of 25 MHz repetition rate micropulses. The FELIX wavelength can be tuned over a large range, 4.3–250 μm, which more than adequately covers the 4.7–5.5 μm range of interest in these experiments. The micropulse length is variable from 300 fs to 5 ps.

The transient grating technique is well-suited to measuring the lifetimes of LVMs. In this technique, the pulsed output of FELIX is split into three parts by two BaF_2 beamsplitters: a "probe" pulse (having wave vector $\mathbf{k}_1$) and two "pump" pulses (having wave vectors $\mathbf{k}_2$ and $\mathbf{k}_3$, respectively). Note that it is the micropulse length which determines the temporal resolution. The macropulse is a consequence of the fact that FELIX is a radio frequency-linac FEL. The $\mathbf{k}_2$ and $\mathbf{k}_3$ pulses are made to spatially and temporally overlap on the sample. If the FEL is resonant with a LVM absorption wavelength, then the excitation of the modes is spatially modulated across the overlap region, resulting in a population grating. The $\mathbf{k}_1$ pulses can then be diffracted from this grating into the phase-matched direction $\mathbf{k}_d=\mathbf{k}_1\pm\mathbf{q}$, where $\mathbf{q}$ is the grating wave vector $\mathbf{k}_2$-$\mathbf{k}_3$, and appropriately detected. Figure 1 displays the transmission geometry (forward box) that was employed in these experiments. Thus by scanning the time delay t of the probe pulses with respect to the pump pulses, the amplitude of the population grating can be measured as a function of time. In these experiments the diffracted pulses were detected by a liquid nitrogen cooled HgCdTe detector and the signals recorded by means of a boxcar integrator.

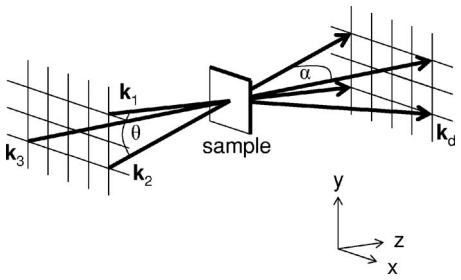

FIG. 1. Schematic diagram of the beam geometry utilized in the transient grating experiment. The experimental values of the angles are $\alpha=16°$ and $\theta=12°$.

The micropulse train is incident upon the sample, however, for all of the lifetime measurements the boxcar integrator is used to gate out an appropriate portion of the macropulse and we therefore integrate the micropulse signals over some time interval. The time interval is chosen to avoid the macropulse buildup time (where the micropulse energy changes rapidly from micropulse to micropulse) and also the decaying end of the macropulse, where the wavelength of the pulses can become unstable. Measurements of the grating decay, where only the leading edge of the macropulse was gated showed no difference to measurements made using any other component of the macropulse.

For the transient grating measurements, the grating period Λ is given by[11]

$$\Lambda = \frac{2\pi}{|\mathbf{q}|} = \frac{\lambda_p}{2\sin(\alpha/2)}, \tag{1}$$

where λ_p is the wavelength of the pump pulses and α is the angle between the two pumps (see Fig. 1). Thus, the grating period is between 18 and 20 μm over the wavelength range that was used in these experiments. The beam diameters were held constant at ~800 μm for the three beams, respectively, thus giving a total of ~35 grating periods in the overlap region. The grating itself is an optically thin refractive index grating with similar overall characteristics to those reported in our earlier work.[10] The grating decays as $\exp(-2t/\langle T_1\rangle)$ and thus the lifetime of the LVMs can be measured. The absorption length of the two modes, deduced from transmission measurements, is ~26 μm for the SiH stretch mode and ~46 μm for the GeH stretch mode.

In order to perform temperature dependent measurements the sample was placed in an Oxford Instruments "microstat" cryostat and connected to an Oxford Instruments model ITC503 temperature controller. Thus the "lattice" temperature could be controlled. There is also a contribution to the temperature from the nonequilibrium bath vibrations that are generated during the relaxation of the excited LVMs. This can lead to a distorted measurement of the lifetime if not properly accounted for: the nonequilibrium phonon population can cause stimulated emission of the LVMs, thus increasing the relaxation rate. As the nonequilibrium population is dependent upon the number of LVMs excited, power dependent measurements of the lifetime are performed to discern at what intensities this effect begins to contribute to the relaxation rate. For the measurements presented here, a total pump energy of not more than 1.3 μJ is employed.

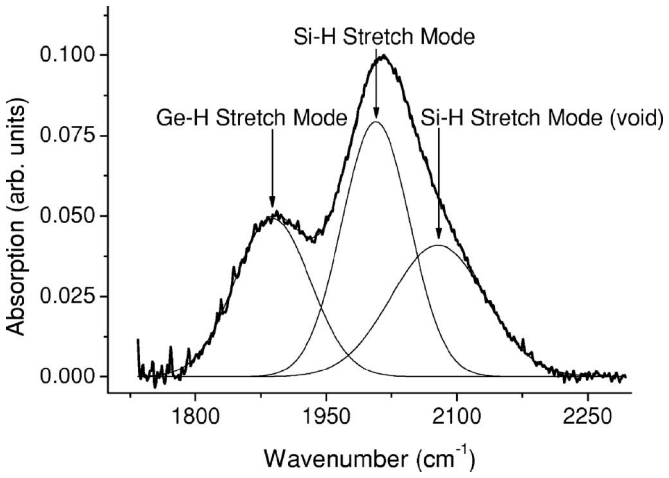

FIG. 2. 10 K infrared transmission spectrum of an *a*-SiGe:H thin film showing the Si–H and Ge–H stretch modes.

Further, gating both at the start and the end of the macropulse with a gate width of 0.5 μs yielded no discernable difference in the lifetimes recorded.

III. RESULTS AND DISCUSSION

Figure 2 displays the relevant portion of the mid-infrared absorption spectrum of the *a*-SiGe:H film. Decomposition of the large absorption feature between 1800 and 2200 cm^{-1} into its constituent Gaussian components show there to be three peaks with resonant frequencies at 1880, 2000, and 2080 cm^{-1}. From previous measurements in the literature,[12,13] these modes can be ascribed to the Ge-H stretching mode (at 1880 cm^{-1}), the Si–H stretching mode (at 2000 cm^{-1}) and a contribution at 2100 cm^{-1} due to the stretching mode of Si–H bonds when this complex is located on an internal void surface and/or the presence of $Si–H_2$ dihydride groups. The large linewidths of these absorption features are characteristic of vibrational modes in an amorphous environment and are due to significant inhomogeneous broadening from the amorphous host.

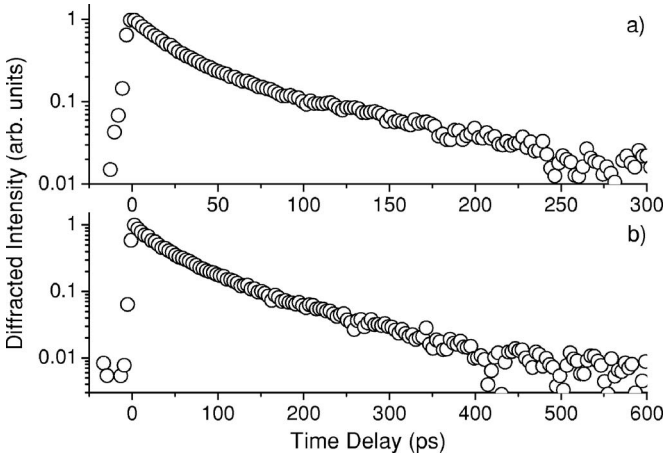

FIG. 3. 10 K transient grating signals when resonantly exciting (a) the Ge–H stretch mode at 5.32 μm and (b) the Si–H stretch mode at 5.00 μm.

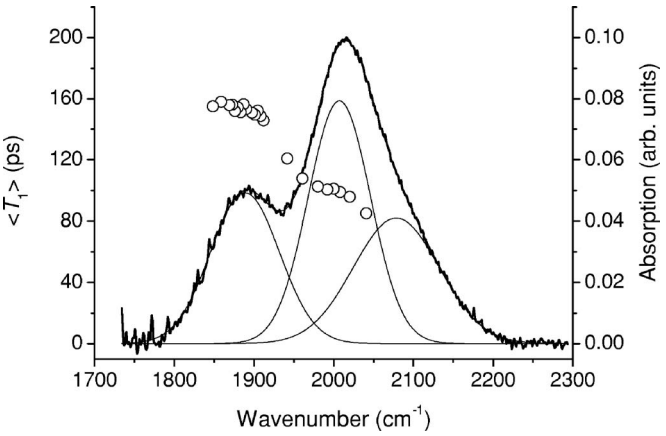

FIG. 4. Wavelength dependent lifetimes superimposed on the linear transmission spectrum.

Figure 3 displays the time integrated transient grating signals when the wavelength of the FEL is resonant with (a) the Si–H and (b) Ge–H stretching modes. It is immediately apparent that both traces are nonexponential, as is observed when the Si(Ge):H complexes are situated in the native amorphous environment. As the nonexponentiality is due to a distribution of lifetimes, it is not possible to fit a curve to the data and obtain an absolute value for the lifetime. Instead, an ensemble averaged lifetime is inferred, which is defined as

$$\langle T_g \rangle = \int tS_g(t)dt \Big/ \int S_g(t)dt, \tag{2}$$

where T_g is the decay time of the population grating, t is the time delay, and S_g is the diffracted intensity. The lifetime of the mode T_1 is related very simply to T_g by the relation $\langle T_1 \rangle = 2\langle T_g \rangle$. In this way, the mean lifetimes of the Si–H and Ge–H stretching modes were measured (at 10 K) to be 101 and 154 ps, respectively.

Figure 4 displays measured average lifetimes as the FELIX wavelength is scanned across the absorption spectrum of the Si(Ge)-H stretch modes. Starting with the lifetimes in the vicinity of the Ge-H stretch mode, it is seen that the lifetime of the mode does not appreciably change on the red side of the absorption feature. However as the excitation wavelength is decreased, the measured value of $\langle T_1 \rangle$ decreases as the spectral overlap with the Si–H stretch mode increases. A small plateau is reached at a spectral position that is just to the low energy side of the peak of the stretch mode. This position is from where we assign the $\langle T_1 \rangle$ of the Si–H stretch mode. As the wavelength is shifted further toward higher energies, the measured $\langle T_1 \rangle$ begins to fall again, this time due to overlap with the Si–H stretch mode associated with hydrogen bonded to the surface of inner voids and/or multihydride species. A similar effect has been reported by Rella *et al.* for the Si–H stretch mode in *a*-Si:H.[14] The wavelength dependence of the lifetimes in the region of the Si–H stretch mode is similar to that measured in *a*-Si:H, however, the absolute magnitude of the lifetimes are markedly different. The average lifetime of the Si–H stretch mode is 138 ps in *a*-Si:H,[6] a result we have confirmed. The reduction in $\langle T_1 \rangle$ of the Ge-H stretch mode in *a*-SiGe:H is even

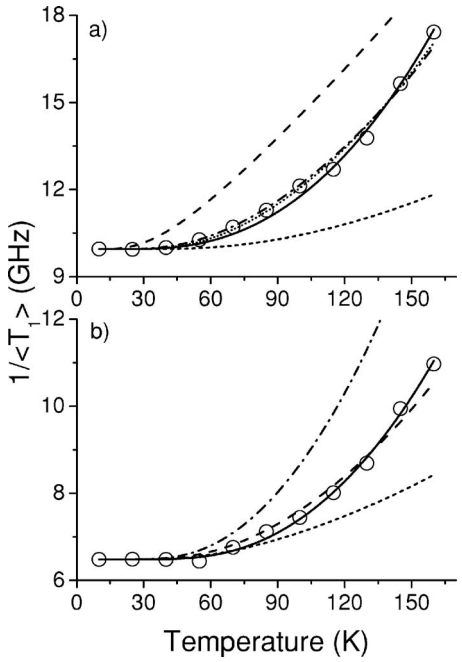

FIG. 5. Temperature dependent mean population decay rates of (a) the SiH stretch mode and (b) the GeH stretch mode. The open circles are the measured values and the curves represent various fits to Eq. (2). The three best fits in plot (a) correspond to relaxation to: one Si–H bending mode, four Si–Si 301 cm^{-1} LA phonons, and one Si–Si 154 cm^{-1} TA phonon (unbroken curve); two Si–H bending modes, a Si–Ge 385 cm^{-1} TO phonon and two Si–Si 168 cm^{-1} TA phonons (dotted curve); one Si–H bending mode, two Si–Si 505 cm^{-1} TO phonons, one Si–Si 214 cm^{-1} TA phonon, and one Si–Si 136 cm^{-1} TA phonon (dashed-dotted curve). The two best fits in plot (b) correspond to relaxation to: one Ge–H bending mode, four Ge–Ge 294 cm^{-1} TO phonons, and one Ge-Ge 132 cm^{-1} TA phonon (unbroken curve); two Ge-H bending modes, one Si–Ge 441 cm^{-1} TO phonon, and two Ge–Ge 150 cm^{-1} LA phonons (dashed curve).

more pronounced: the lifetime of this mode is 306 ps in *a*-Ge:H.[8] Thus, we deem it highly likely that the presence of mixed character Si–Ge vibrations increases the number of possible relaxation channels, thereby reducing the lifetime.

Temperature dependent measurements of $\langle T_1 \rangle$ allow a direct assessment of the decay channels to be made. Figures 5(a) and 5(b) display the temperature dependence of the averaged decay rate of the Si–H and Ge–H modes, respectively. The measured rates increase by factors of approximately 1.7–1.9 as the temperature increases from 10 to 155 K, due to stimulated phonon emission. The dependence of the anharmonic decay rates on temperature is given by[15]

$$[T_1(T)]^{-1} = [T_1(0)]^{-1}\left\{\frac{\exp(\hbar\omega/k_BT)-1}{\Pi_i[\exp(\hbar\omega_i/k_BT)-1]}\right\}, \qquad (3)$$

where $T_1(0)$ is the lifetime at a temperature of 0 K, which we have approximated by our 10 K measurement, ω is the frequency of the excited mode and ω_i the frequencies of the accepting modes fulfilling the energy-conserving relation $\Sigma_i \hbar\omega_i = \hbar\omega$.

Figure 5(a) displays the temperature dependence of the lifetime of the Si–H stretching mode. The short-dashed curve represents anharmonic decay into two Si–H bending modes of the Si:H complex at 640 cm^{-1},[13] one Si–Si TO phonon at 505 cm^{-1} and another Si–Si transverse acoustic (TA) phonon at 215 cm^{-1}. This trend completely underestimates the rise in the relaxation rate as the sample temperature increases, due to the high energy of the bulk vibrations. Conversely, the dashed curve shows decay to three Si–H bending modes and one 80 cm^{-1} phonon which overestimates the increase in relaxation rate due to the low energy of the 80 cm^{-1} phonon. The remaining three curves are reasonable approximations to the experimental data. The solid line shows sixth order decay into one Si–H bending mode, four Si–Si longitudinal acoustic (LA) phonons at 301 cm^{-1} and one Si–Si TA phonon at 154 cm^{-1}. The dotted line represents five phonon decay into two Si–H bending modes, a Si–Ge TO phonon at 385 cm^{-1}, and two Si–Si 168 cm^{-1} TA phonons. Finally, the dashed-dotted curve represents decay to one Si–H bending mode, two Si–Si TO phonons at 505 cm^{-1}, and two Si–Si TA phonons: one at 214 cm^{-1} and at the other at 136 cm^{-1}. The dotted and dashed-dotted curve fit the data most closely. The key difference between the two relaxation pathways is that the dotted curve represents a pathway by which some of the vibrational energy is deposited into the mixed character Si–Ge vibrational modes. Considering that the same LVMs and lattice modes are available to decay to in the pure *a*-Si:H system and that there is a clear difference in $\langle T_1 \rangle$ in that case, it would seem that the more likely relaxation pathway is the one whereby relaxation is partly via the Si–Ge vibrational modes themselves.

Figure 5(b) displays the temperature dependent measurements of the average relaxation rate of the Ge-H stretching mode. The short-dashed curve illustrates relaxation into four accepting modes: three Ge-H bending modes at 570 cm^{-1} (Ref. 12) and one Ge-Ge 170 cm^{-1} LA phonon. This underestimates the increase in the relaxation rate as a consequence of the high phonon energies involved. The dashed-dotted curve represents anharmonic decay into two Ge-H bending modes and four 214 cm^{-1} phonons, which overestimates the increase in the decay rate. Raman scattering studies indicate that these phonons at 214 cm^{-1} are resonant vibrational mode, the identity of which is yet to be ascertained.[16] There are two assumptions which closely approximate the data. The solid curve represents a six phonon decay process having accepting modes comprising one Ge-H bending mode, four Ge-Ge TO phonons at 294 cm^{-1} (Ref. 17), and one Ge-Ge TA phonon at 132 cm^{-1}. The dashed curve represents relaxation to two Ge-H bending modes, a Si–Ge TO phonon at 441 cm^{-1}, and two Ge-Ge LA phonons at 150 cm^{-1}.

These temperature dependent measurements show that both the Si–H and Ge–H stretch mode have the possibility of relaxing by depositing some of their vibrational energy into the Si–Ge vibrational modes and it is almost certain that inclusion of such mixed states is chiefly responsible for the reduction in lifetime as compared to the Si(Ge)–H stretch mode in *a*-Si(Ge):H. The reduction in the lifetime is most significant for the Ge-H mode. When the Ge:H complex is situated in a pure *a*-Ge matrix, the phonon cutoff is close to 320 cm^{-1}, however, in *a*-SiGe the phonon cutoff is near 460 cm^{-1}. Thus the bulk vibrational density of states observed by the Ge-H mode in *a*-SiGe provides for a significantly greater number of possible relaxation pathways and

explains the factor of 2 increase in the 10 K decay rate. This suggests the dashed curve in Fig. 5(b) is the most likely decay route.

IV. CONCLUSION

Temperature dependent measurements of the lifetime of the Si–H and Ge–H stretching mode of the Si(Ge):H complexes in an *a*-SiGe:H thin film have been performed using the transient grating technique in a forward box geometry with excitation provided by the pulsed output of a FEL. The decay of both modes has been demonstrated to be multiexponential, confirming the importance of the local environment of the "defect" center in causing a distribution of relaxation rates. Analysis of the temperature dependence of the lifetimes shows that the relaxation of both modes proceeds via the Si(Ge)–H bending modes, with the energy gap bridged by the phonon bath of the host material and that the stretching modes can decay both via Si(Ge)–Si(Ge) and mixed Si–Ge vibrations. Comparison with previously measured values of $\langle T_1 \rangle$ of the Si(Ge)–H stretching modes in either *a*-Si or *a*-Ge leads us to conclude that the reduction in lifetime is attributable to the inclusion of the mixed states in the phonon bath of the *a*-SiGe amorphous matrix.

ACKNOWLEDGMENTS

The authors acknowledge the support of the Dutch FOM (Stichting voor Fundamenteel Onderzoek der Materie) organization in providing the required beamtime on FELIX as a part of the FOM-EPSRC-GB agreement and would like to thank the FELIX staff for their skillful assistance. K.W.J. would like to thank the British Engineering and Physical Sciences Research Council (EPSRC-GB) for providing a DTA studentship. We would also like to thank Karine van der Werf for preparing the *a*-SiGe:H samples.

[1] G. Conte, D. Della Sala, F. Galuzzi, G. Grillo, C. Ostrifate, and C. Reita, Semicond. Sci. Technol. **5**, 890 (1990).
[2] Y.-P. Chou and S.-C. Lee, J. Appl. Phys. **83**, 4111 (1998).
[3] A. Skumanich and N. M. Amer, J. Non-Cryst. Solids **59–60**, 249 (1983).
[4] V. L. Dalal, Y. Liu, Z. Zhou, and K. Han, J. Non-Cryst. Solids **299–302**, 1127 (2002).
[5] V. Chu, J. P. Conde, S. Aljishi, and S. Wagner, Mater. Res. Soc. Symp. Proc. **118**, 167 (1988).
[6] M. van der Voort, C. W. Rella, L. F. G. van der Meer, A. V. Akimov, and J. I. Dijkhuis, Phys. Rev. Lett. **84**, 1236 (2000).
[7] Z. Xu, P. M. Fauchet, C. W. Rella, H. A. Schwettman, and C. C. Tsai, J. Non-Cryst. Solids **198–200**, 11 (1996).
[8] K. W. Jobson, J.-P. R. Wells, R. E. I. Schropp, P. J. Phillips, and J. I. Dijkhuis, Phys. Rev. B **73**, 155202 (2006).
[9] J.-P. R. Wells, R. E. I. Schropp, L. F. G. van der Meer, and J. I. Dijkhuis, Phys. Rev. Lett. **89**, 125504 (2002).
[10] J.-P. R. Wells, P. J. Phillips, N. Tomozeiu, F. H. P. M. Habraken, and J. I. Dijkhuis, Phys. Rev. B **68**, 115207 (2003).
[11] H. J. Eichler, P. Günter, and D. W. Pohl, *Laser Induced Dynamic Gratings* (Springer, Berlin, 1986).
[12] D. Bermejo and M. Cardona, J. Non-Cryst. Solids **32**, 421 (1979).
[13] M. H. Brodsky, M. Cardona, and J. J. Cuomo, Phys. Rev. B **16**, 3556 (1977).
[14] C. W. Rella, M. van der Voort, A. V. Akimov, A. F. G. van der Meer, and J. I. Dijkhuis, Appl. Phys. Lett. **75**, 2945 (1999).
[15] A. Nitzan, S. Mukamel, and J. Jortner, J. Chem. Phys. **60**, 3929 (1974).
[16] J. S. Lannin, Phys. Rev. B **16**, 1510 (1977).
[17] S. C. Shen, C. J. Fang, M. Cardona, and L. Genzel, Phys. Rev. B **22**, 2913 (1980).